Network Dependence of the Dilemmas Of Cooperation

J. M. Pacheco[1,2] and F. C. Santos[2]

[1] Centro de Física Teórica e Computacional and Departamento de Física da Faculdade de Ciências, Complexo Interdisciplinar da Universidade de Lisboa, P-1649-003 Lisboa Codex, Portugal
[2] GADGET, Apartado 1329, P-1009-001 Lisboa, Portugal

Abstract. Evolutionary game theory has become a powerful framework to investigate the evolution of cooperation. Games such as the prisoner's dilemma or the snowdrift game are frequently used to model cooperation, and to study its emergence in the context of Darwinian evolution. Until recently, spatial structure was understood as one of the main mechanisms helping the sustainability of cooperation. However, recent results for the snowdrift game have cast serious doubts on the general applicability of this result. Here we show that cooperation may become the dominating strategy, *both* for the prisoner's dilemma *and* the snowdrift game, depending on the underlying network of contacts between individuals. By recasting the problem in the framework of graph theory, and associating to the network of contacts graphs of Small-World and Scale-Free type, we demonstrate that graphs exhibiting power-law degree distributions resulting from the mechanisms of growth and preferential attachment provide excellent conditions for cooperation to dominate. These results apply from very large population sizes down to communities with nearly one hundred individuals.

INTRODUCTION

Cooperation is an essential ingredient of evolution. We know that animals cooperate in families to raise their offsprings and in groups, to prey as well as to reduce the risk of predation. However, understanding the emergence of cooperation in the context of Darwinian evolution remains a challenge to date. The theory of reciprocal altruism, set forward by Trivers[1] in 1971, has been formalized ten years later by Axelrod and Hamilton[2] using an evolutionary game-theoretic[3,4] model of the repeated Prisoner's Dilemma (**PD**). In the **PD**, the fitness advantage of defectors makes such strategies evolutionary stable. As such, numerous studies have been carried out in order to elucidate the mechanisms responsible for the persistence of cooperative behaviour, thereby resolving the apparent contradiction between the elementary predictions of the game and empirical evidence. Among the different possibilities, it has become well established[5,6,7] that incorporation of spatial structure in the **PD** acts to enhance cooperation, since spatial structure allows the formation of clusters of cooperators which may acquire the necessary "critical size" and resist invasion by defectors.

Recently[8] the demonstration that, in the Snowdrift Game (**SG**), incorporation of spatial structure may inhibit cooperation brought onto questionable grounds the conventional wisdom emanating from the **PD** studies, a feature which is more worrisome in view of

the observation that several biological communities may engage in games other than the **PD**, such as the **SG** or other hawk-dove type games[8-11].
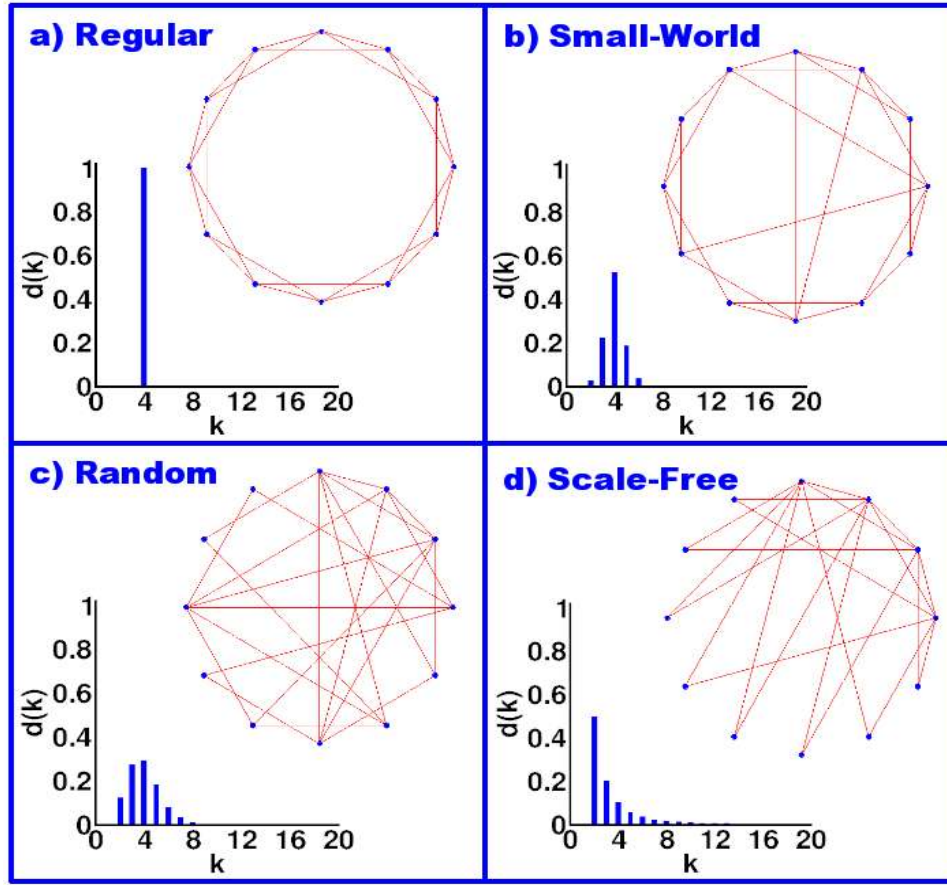
FIGURE 1. Different **NOCs a)** Regular graph with N =12 vertices each of which has z = 4 edges. z = N-1 leads to a fully-connected graph. **b)** Small-World graph, generated from **a)** using the value *0.2* for the rewiring probability p_{SW} (see main text for details). **c)** Random graph, obtained in the limit p_{SW} = *1*. **d) SF** graph, generated using model of Barabasi and Albert for m = m_0 = 2 (see methods); **Histograms :** Degree distributions *d(k)* computed for each type of graphs and N=10^4; *d(k)*= N_k / N, where N_k gives the number of vertices with k edges. In all cases the average connectivity z of the graphs is *4*.

Up to now, however, studies of the evolution of cooperation have been mostly carried out in two extreme scenarios: Purely unstructured populations (well-mixed limit, also known in physics as the mean-field approximation) and "spatially structured" populations. In the language of graph theory both situations may be associated with regular graphs (Fig. 1-a), the well-mixed limit taking place for the fully connected graph. At variance with Fig. 1, spatial structure is typically implemented on so-called 2d-lattices, such as a square lattice, in which individuals are constrained to interact solely with their closest neighbours, typically the "nearest" 4 or 8, defining also a regular Network Of Contacts (**NOCs**). All these types of regular graphs share the same degree distribution *d(k)* (defined for a graph with N vertices as *d(k)*= N_k / N, where N_k gives the number of vertices with k edges), which is given by $\delta(k$- $z)$, where z is the degree (number of edges) of each vertex. As increasingly recognized[12-16], both scenarios constitute rather unrealistic representations of real world **NOCs**, which one intuitively

associates with intermediate situations, in which "spatial structure" coexists with "long-range" connections, or shortcuts (Figs. 1-c and 1-d). Indeed, such topologies are characteristic of a plethora[15,16] of everyday natural, social and technological networks, and as such we expect them to play a role in the evolution of cooperation. The "Small-World" graphs (**SW**) of Watts and Strogatz[12] (Fig. 1-c) provide one possibility of accounting for such scenarios, although they lack the power-law degree distribution so characteristic[13-16] of real-world **NOCs**. Such a feature is easily obtained with the Scale Free (**SF**) graphs of Barabasi and Albert[13] (Fig. 1-d). Here we recast the study of the evolution of cooperation as encapsulated in the **PD** and the **SG** games in communities in which the **NOCs** are associated with graphs of **SW** and **SF** types.

METHODS

Networks Of Contacts

Starting from a regular ring (Fig. 1-a), for a fixed number N of elements of the community (vertices of the graph) and for a given number of connections z per vertex (edges of the graph), we generate a **SW** graph by rewiring, with probability p_{SW}, each edge of the graph. Rewiring means here replacing the original edge maintaining its origin and choosing randomly the ending vertex, such that self-connections – loops – and double connections are excluded. At the end of the rewiring process, one no longer has a single peak degree distibution, but still one has an average value of the degree distribution $<d(k)>$ given by z.

Besides the degree distribution $d(k)$, the probabilistic nature of the construction of **SW** (and **SF**, see below) graphs leads to many different realizations of **NOCs** for given values of the parameters. Consequently, other quantities provide additional information[15,16] which characterizes a given class of **NOCs** namely, the average path length L, providing the number of edges in the shortest path between two vertices, averaged over all pairs of vertices, and the cluster coefficient C, which provides a measure of the extent to which direct neighbours of a given vertex are direct neighbours of each other, being roughly proportional to the number of such triangular connections. For the **SW** graphs, small values of $p_{SW} > 2/(zN)$ ensure large values of $C \sim C_{regular} \sim (3z-6)/(4z-4)$ and small values of $L \sim L_{random} << L_{regular} \sim N/z$, characteristic of the **SW** regime, whereas as $p_{SW} \rightarrow 1$ we fall in the limit of a random graph, for which $C_{random} \sim z/N$ and $L_{random} \sim ln(N) / ln(z)$ are both small.

On the other hand, the construction of a **SF** graph involves two processes: *1- Growth*: Starting with a small number (m_0) of vertices, at every timestep we add a new vertex with $m \leq m_0$ edges that link the new vertex to m different vertices already present in the system; *2- Preferential attachment*: When choosing the vertices to which the new vertex connects, we assume that the probability p_i that a new vertex will be connected to vertex i depends on the degree k_i of vertex i: $p_i = k_i / \Sigma k_i$. After t timesteps this algorithm produces a graph with $N = t + m_0$ vertices and mt edges. We have also tested one variant [14] of this SF model, in which the preferential attachment probability p_i is replaced with a uniform attachment probability. For the less studied **SF** graphs, typically[15,16] $C \sim C_{random}$ whereas $L \sim ln(N)/ln[ln(N)]$, reflecting the ultra-small [17] nature of these networks.

Games

In the simple, one-shot **PD** adopted here, individuals are either cooperators or defectors, acting accordingly whenever two of them interact. They both receive R upon mutual cooperation and P upon mutual defection. A defector exploiting a cooperator gets an amount T and the exploited cooperator receives S, such that $T > R > P > S$. On the other hand, in the **SG**, we have $T > R > S > P$. Thus, at variance with the **PD**, for which it is best to defect regardless of the opponent's decision, in the **SG** the best action depends on the opponent: to defect if the other cooperates, but to cooperate if the other defects. This leads to a different evolutionary behaviour for the two games[8]. In particular, for the **SG** played in infinite, well-mixed populations, that is, for an underlying fully connected graph, and following replicator dynamics[18], the equilibrium frequency of cooperators is given by $1 - r$, with r the cost-to-benefit ratio of mutual cooperation (defined below). Following common practice[5,8], we start by rescaling the games such that each depends on a single parameter. For the **PD**, we make $2 > T = b > 1$, $R = 1$ and $P = S = 0$, where b represents the advantage of defectors over cooperators[5]. For the **SG**, we make $T = \beta > 1$, $R = \beta - 1/2$, $S = \beta - 1$ and $P = 0$, such that the cost-to-benefit ratio of mutual cooperation can be written as $r = 1/(2\beta - 1)$, with $0 \leq r \leq 1$.

Simulations

Individuals are placed on the vertices of graphs with $N = 10^4$ vertices; we use periodic boundary conditions for the regular ring graphs and the values $z \geq 4$, $0 \leq p_{SW} \leq 1$ and $m = m_0 \geq 2$ ($z = \langle d(k) \rangle = 2m_0$). Following Hauert & Doebeli[8], equilibrium frequencies of cooperators and defectors are obtained by averaging over 1000 generations after a transient time of 10000 generations, starting from an equal distribution of strategies among the elements of the population. We confirmed that averaging over larger periods or using different transient times did not change the results, although the transient period depends on the characteristic path length of the system, which in turn depends on z, N, and p_{SW}. For different values of the parameters, the evolution of the frequency of cooperation as a function of r for the **SG** and b for the **PD** has been computed. To this end, each data point in the Figures results from an average over 20 realizations of the same type of **NOCs** specified by the appropriate parameters (N, z, p_{SW} and $m = m_0$).

Evolution

The following transition probabilities constitute the finite population analogue of replicator dynamics[8], to which simulation results converge in the limit of well-mixed populations. In each generation, all pairs of individuals x and y, directly connected, engage in a single round of a given game, their accumulated payoffs being stored as P_x and P_y, respectively. Whenever a site x is updated, a neighbour y is drawn at random among all k_x neighbours; whenever $P_y > P_x$ the chosen neighbour takes over site x with probability given by $(P_y - P_x)/(D k_>)$, where $k_>$ is the largest between k_x and k_y and $D = T - S$ for the **PD** and $D = T - P$ for the **SG**.

RESULTS

Fig.2 shows the results of our simulations for the **PD** and the **SG**, respectively, evolving on regular ring-graphs for different values of z. They confirm the results obtained by Hauert and Doebeli[8] on 2d-lattices.
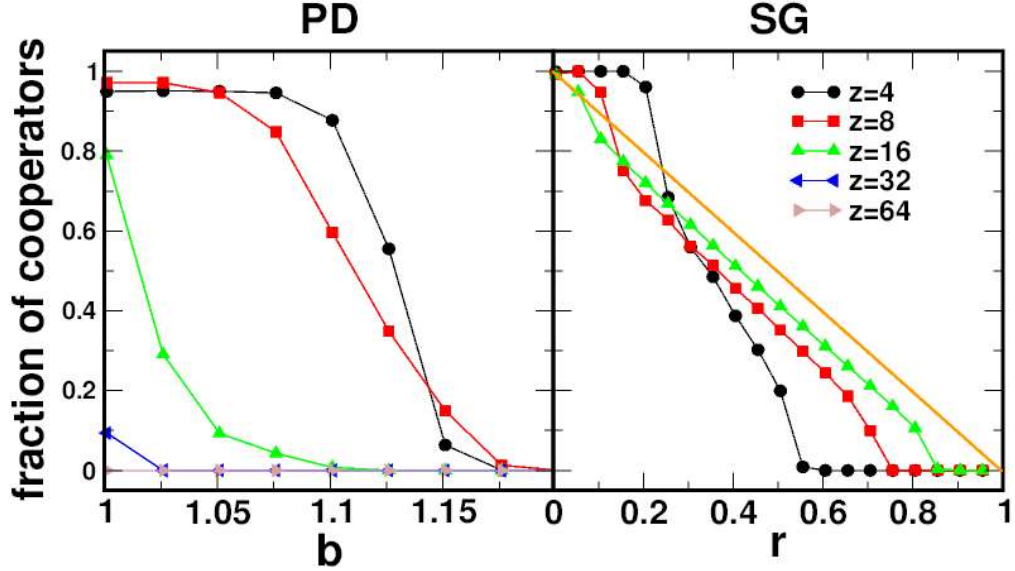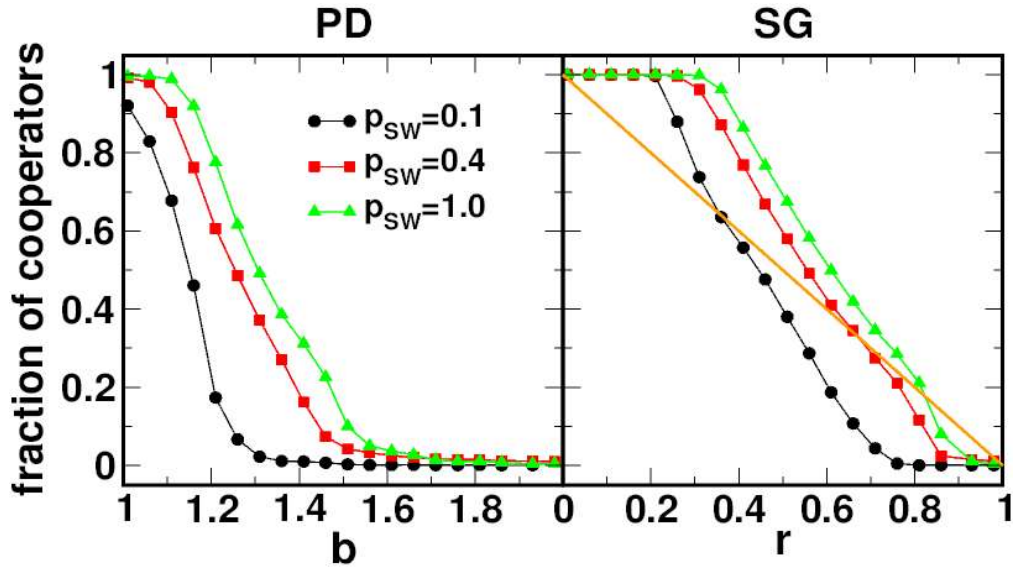

FIGURE 2. Fraction of cooperators for regular **NOCs** and different values of z. **Left panel**: Results for the **PD** are plotted as a function of the temptation to defeat b. **Right panel**: Results for the **SG** are plotted as a function of the cost to benefit ratio r (see main text for details).

Furthermore, they show how z influences the evolution of cooperation on regular **NOCs**. Indeed, deviations from the well-mixed population limits are more pronounced the smaller the value of z. Moreover, from Fig. 2 it is clear that for $z = 64$ the well-mixed limit has already been reached for the **PD**. On the other hand, for the **SG** that limit will only be reached whenever $z \sim N\text{-}1$ (we confirmed that the well-mixed limit is also obtained for the **SG**).

Fig. 3 shows what happens as one moves away from regularity for the **NOCs**, such that $d(k)$ is not anymore a delta distribution (we consistently interpret z as $<d(k)>$, the average value of the degree distribution). In the interval $2/(zN) \leq p_{sw} \leq 0.1$, in the **SW** regime, the shape of the curve for the frequency of cooperation gets gradually smoother with increasing p_{sw}, for both games, up to the shape shown for $p_{sw} = 0.1$. As one increases p_{sw} inside this interval the value of L drops significantly compared to $L_{regular}$, whereas $C \approx C_{regular}$. For $0.1 \leq p_{sw} \leq 1.0$, L remains small ($L \approx L_{random}$) whereas C drops significantly. For large p_{sw} we observe an overall enhancement of cooperation, in **both** games, over a wide range of the corresponding parameters, which constitutes a remarkable result, at odds with previous studies[5,8].
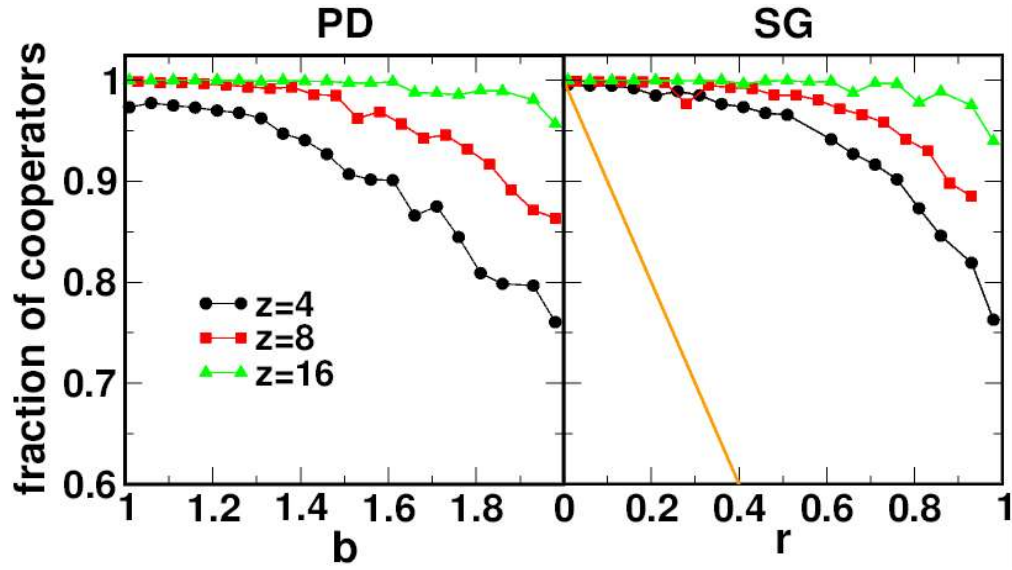
FIGURE 3. Fraction of cooperators for the **SW NOCs** of Watts and Strogatz, for different values of p_{sw}. **Left panel**: Results for the **PD** are plotted as a function of the temptation to defeat b. **Right panel**: Results for the **SG** are plotted as a function of the cost to benefit ratio r. An overall enhancement of cooperation is observed, for both games, with respect to the well-mixed limit and regular graphs, although cooperation is best sustained for small values of b and r.

Similarly to $p_{sw}=0$, we observe that the deviations from the well-mixed results get smaller as we increase z, approaching the well-mixed population limit as $z \rightarrow N\text{-}1$. As such, for $p_{sw}=1$ and $z=4$ we get the maximal deviations from the well-mixed results.

Fig. 4 shows the corresponding results for a **SF NOCs**, for $z = m/2 = m_0/2 \geq 4$, exhibiting a completely different behaviour: Cooperation dominates in ***both*** games and for ***the entire*** domain of parameters b and r, which constitutes an unprecedented result[19]. On the folllowing we elucidate the mechanisms on the basis of these results as well as the dependence of such results on the community size N.

Besides the small values of C and L, graphs of **SF** type exhibit a power law scaling of the degree distribution, such that many vertices have a very small connectivity, whereas a few vertices act as hubs, with a high degree of connectivity. The occurrence of these hubs results from the preferential attachment rule. As such, we investigate the impact of preferential attachment (and of growth, see below) in the evolution of cooperation.
To this end we modify[14] the rules of construction of the **SF** graphs by replacing the preferential attachment rule by a uniform attachment rule. We compare the results of both models generated with $m = m_0 = 2$ with those obtained with **SW** graphs with $p_{sw} =1$ and $z = 4$, which provide a possible limit to which the **SF** evolve whenever growth and preferential attachment are not included.

FIGURE 4. Fraction of cooperators for the **SF NOCs** of Barabasi and Albert, for different values of *z*. **Left panel**: Results for the **PD** are plotted as a function of the temptation to defeat *b*. **Right panel**: Results for the **SG** are plotted as a function of the cost to benefit ratio *r*. Contrary to previous results, cooperation dominates for the whole ranges of *b* and *r* on **SF** graphs. Contrary to the results for regular graphs, cooperation gets enhanced with increasing *z*, up to a critical value, above which cooperation collapses, rapidly approaching the well-mixed limit.

Fig. 5 shows the impact of the different rules on the evolution of cooperation for both the **PD** and the **SG**. Results show that both processes are important in what concerns the evolution of cooperation.

Preferential attachment is mainly responsible for the prevalence of cooperation for unfavourable values of the game parameters, but the role of growth cannot be overlooked and contributes, in a sizeable way, for establishing cooperation as an overall dominating strategy in both games. Yet, the emergence of "hubs" due to preferential attachment, together with the intricate vertex correlations built up during graph generation, which ensures that "hubs" get directly connected to each-other, provide the right mechanisms which turn cooperation into the dominating strategy on both games.
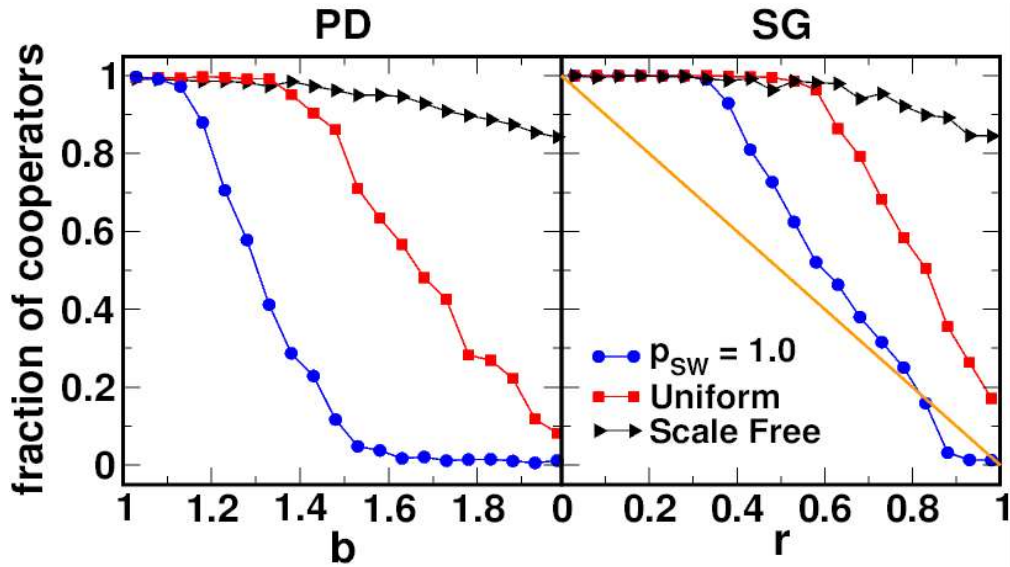
FIGURE 5. Impact of preferential attachment and growth on the evolution of cooperation. **Left panel**: Results for the **PD** as a function of the temptation to defeat *b*. **Right panel**: Results for the **SG** as a function of the cost to benefit ratio *r*. Solid triangles show results for the standard **SF** model, solid squares show results the **SF** model with uniform attachment and solid circles show results for **SW** graphs with $p_{SW}=1$. Both growth and preferential attachment are necessary to ensure the dominance of cooperation, for both games and throughout the entire parameter ranges.

Evolution Of Cooperation On Small Communities

We finally investigated the dependence of the results on the population size *N*, for *z = 4*. We repeated the simulations, progressively reducing the population size. We were able to obtain stable results, qualitatively identical to those shown in Figs. 2-5, down to *N=128*, as shown in Fig. 6 for populations with sizes *N=512* and *N=128*.

The results in Fig. 6 clearly demonstrate that the evolution of cooperation in small communities evolves very much in the same way as it does in much larger ones. It is noteworthy that for such small values of *N* the degree distribution associated with **SF** graphs is not at all scale-free. Yet, growth and preferential attachment "cooperate" to induce vertex correlations which lay the grounds for cooporation to dominate. For values of *N* smaller than *N ≈ 100*, the averages over many realizations of graphs of a given type do not converge to a well defined value, a feature which is not surprising, taking into account the probabilistic rules of construction of those graphs. Indeed, for small values of *N*, stochastic extinction of cooperators happens for particular realizations of a given **NOCs**, as such precluding a clearcut result for the evolution of cooperation. This feature is a size effect which clearly disappears for large *N*.
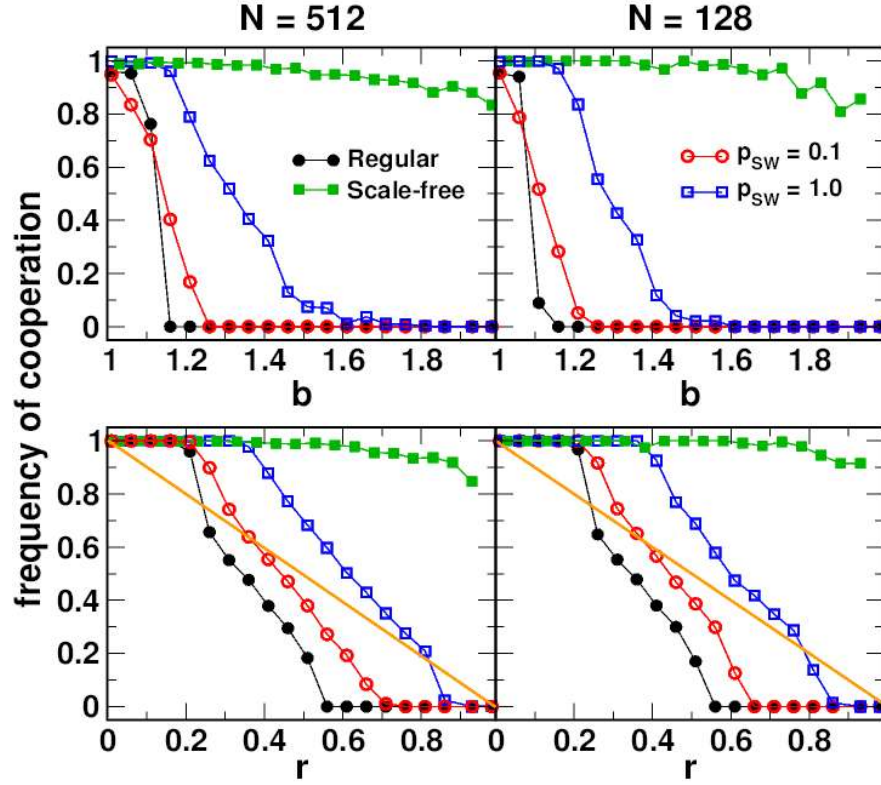
FIGURE 6. Evolution of Cooperation on small communities. Simulations were carried out for *N=512* (left panels) and *N=128* (right panels). In all cases *z=4*. Upper panels: Results for the **PD**. Lower panels: Results for the **SG**. Comparison between these results and those of Figs. 2-5 show that the qualitative features of the evolution of cooperation remain the same. For *N=128* the oscillations at high values of *b* in the PD game indicate that, for such values at which competition between defectors and cooperators takes place more effectively, the small population size enhances the dependence of cooperation on the particulars of each realization of a **NOCs**.

Hub Dynamics

In the well-mixed limit we know that a single defector placed in an otherwise cooperative population will ultimately invade the entire population. For **SF NOCs**, it is easy to convince oneself that the best location for placing a single defector is on the hub with largest connectivity. Starting from this scenario, the evolutionary dynamics is startling, as shown in Fig. 7, for *N=10⁴*, *z=4* and *b={1.1,1.5,1.9}*, in which we plot the evolution of the fraction of direct neighbours of the defecting hub which are cooperators. The initial defector quickly invades the nearest (cooperative) neighbours, reducing their frequency to roughly 20%. However, the invaded neighbours are mostly individuals with low connectivity, since other hubs, initially populated with cooperators, will resist invasion by the initial defector, due to their high fitness resulting from many mutual cooperative interactions. After a few generations the original defector has less and less cooperators to exploit, which reduces its fitness, thereby becoming more susceptible for being invaded by a directly connected cooperator located in a nearby hub. Indeed, cooperator invasion originates preferentially from hubs. Incidentally, hubs with lower connectivity may be invaded by defectors, but will be re-occupied by

cooperators at a later stage.

The overall result is that the original defector invariably gets replaced by a cooperator. Indeed, we never obtained a situation in which the defector was able to survive. In order to provide the initial defector with the capacity to invade the whole population, one needs to increase the value z, since beyond a critical value (which depends on N and b) the dynamics of evolution will reduce to the well-mixed limit. As noted before, the inter-connectedness of hubs plays an important role, and this is a feature which arises naturally in the scale free model of Barabasi and Albert, ensuring the sustainability of cooperation.
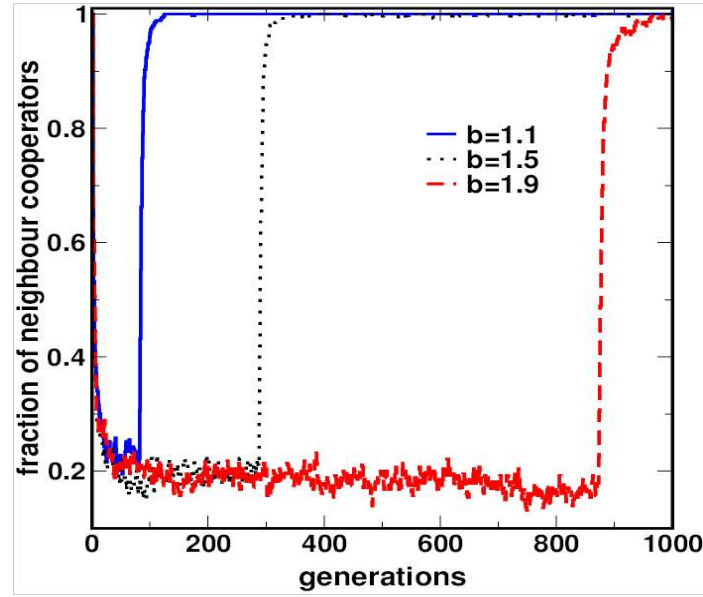
FIGURE 7. Evolution of cooperators around largest hub. Starting with a single defector placed in the hub with largest connectivity, the fraction of direct neighbours who are cooperators is computed throughout evolution, for a population of $N = 10^4$ individuals and $z = 4$, and for the three values of b indicated. The overall behaviour, independent of b, shows that the initial defector invades approximately 80% of its immediate neighbours, after which the largest hub is invaded by a cooperator (originating from a connected hub, taking place right before each jump), leading to a rapid saturation of the hub's neighbours with cooperators. In what concerns this dynamical behaviour, b acts to increase the amount of time necessary for the largest hub to be invaded by a cooperator.

CONCLUSIONS

Cooperation is very sensitive to the underlying **NOCs** on which it evolves. Different **NOCs** may determine completely different fates for the evolution of cooperation. As such, their role cannot be overlooked, since the underlying topology of the **NOCs** may render cooperation the dominating trait throughout evolution. We hope the present results will stimulate further studies of the impact of the **NOCs** on the evolution of cooperation in particular, and evolutionary game theory in general. For instance, it is clear that the criteria for evolutionary stability in finite populations recently defined[11] should be re-examined in light of the present results.

ACKNOWLEDGMENTS

REFERENCES

1. Trivers, R. The evolution of reciprocal altruism*, Q. Rev. Biol.* 46, (1971) 35-37.
2. Axelrod, R. and Hamilton, W. D., The evolution of cooperation, *Science* 211, 1390 (1981) .
3. von Neumann, J. and Morgenstern, O. *Theory of Games and Economic Behaviour (Princeton Univ. Press, Princeton, 1944)*
4. Maynard Smith, J. *Evolution and the Theory f Games***,** (Cambridge Univ. Press, Cambridge, 1982) .
5. Nowak, M. A. and May, R. M. Evolutionary games and spatial chaos. *Nature* 359, 826–829 (1992) .
6. Killingback, T., Doebeli, M. and Knowlton, N. Variable investment, the continuous prisoner's dilemma, and the origin of cooperation. *Proc. R. Soc. Lond.* B 266, 1723–1728 (1999) .
7. Doebeli, M. and Knowlton, N. The evolution of interspecific mutualisms, *Proc. Natl. Acad. Sci. USA* 95, 8676–8680 (1998).
8. Hauert, Christoph and Doebeli, Michael, Spatial structure often inhibits the evolution of cooperation in the snowdrift game, *Nature* 428, 643-646 (2004).
9. Wilkinson, G. S. and Shank, C. C. Rutting-fight mortality among musk oxen on banks island, Northwest Territories, Canada. *Anim. Behav.* 24, 756–758 (1977).
10. Clutton-Brock, T. H. et al. Selfish sentinels in cooperative mammals. *Science* 284, 1640–1644 (1999). Turner, P. E. and Chao, L. Escape from prisoner's dilemma in RNA phage $\Phi6$. *Am. Nat.* 161, 497–505 (2003).
11. Nowak, Martin A., Sasaki, Akira, Taylor, Christine and Fudenberg, Drew, Emergence of cooperation and evolutionary stability in finite populations, *Nature* 428, 646-650 (2004).
12. Watts, D. J. and Strogatz S. H., Collective dynamics of 'small-world' networks, *Nature* 393, 440–442 (1998).
13. Barabási, A. L., Albert, R., Emergence of scaling in random networks, *Science* 286, 509-512 (1999)*.*
14. Barabási, A. L., Albert, R., Jeong, H. Mean-field theory for scale-free random networks, *Physica A* 272, 173-197 (1999).
15. Albert, R., Barabási, A. L. Statistical mechanics of complex networks, R*eviews of Modern Physics* 74, 47-97 (2002).
16. Dorogotsev, S. N. and Mendes, J. F. F., *Evolution of Networks: From Biological Nets to the Internet and WWW* (Oxford University Press, Oxford, 2003)*.*
17. Cohen, Reuven, and Havlin, Shlomo, Scale-Free Networks are Ultra-Small, *Phys. Rev. Lett. 90*, 058701 (2003).
18. Hofbauer, J. and Sigmund, K. *Evolutionary Games and Population Dynamics* (Cambridge Univ. Press, Cambridge, UK, 1998).
19. Santos, F.C., Pacheco, J. M., Scale-Free Graphs provide a Unifying Framework for the Emergence of Cooperation, (submitted).